

FEM AND EXPERIMENTAL ANALYSIS OF MODE III FRACTURE BEHAVIOR OF COMPOSITE LAMINATES

Youjiang Wang¹ and Dongming Zhao²

¹*School of Textile & Fiber Engineering, Georgia Institute of Technology, Atlanta, Georgia 30332-0295 USA*

²*Johnson Control, Inc., 1005 Pinegrove Drive #204, Holland, Michigan 49423 USA*

SUMMARY: A finite element analysis was performed on a $[90, (+45/-45)_n, (-45/+45)_n, 90]_s$ class of laminated composites under the edge crack torsion (ECT) test configuration. Models were established to study the relations between the interlaminar fracture behavior and various configuration parameters, including the effects of point loads, ends, geometry, Mode II interference, and friction. Results showed that with proper selection of ECT specimen configuration and layup, the delamination could grow in pure Mode III in the middle region of the specimen. An experimental investigation of the mode III fracture behavior of laminated composites was also conducted on carbon/epoxy laminated composites. A new two-point loading fixture was fabricated which was found to be simpler and more versatile than the one-point loading fixture for the ECT test. The results obtained from the test were consistent with those predicted by the finite element analysis.

KEYWORDS: Fracture, Mode III, Testing, FEM, Analysis

INTRODUCTION

Analysis and test techniques for mode I and mode II delamination have been extensively studied. However, relatively less work has been reported for mode III delamination. A mode III test is needed for complete characterization of the three delamination modes to completely describe mixed-mode delamination processes in laminated composites. The edge crack torsion (ECT) test proposed by Lee [1], as shown in Figure 1, is a simple and effective method that could be used for the mode III delamination toughness characterization. This test uses a simple fixture and a rectangular laminated composite specimen with a $[90, (+45/-45)_n, (-45/+45)_n, 90]_s$ class of layups and a midplane free edge delamination under a torsional load. Analyses [1-4] for the ECT test configuration have been carried out, but they generally lack necessary validation since they are based on the significant simplification of loading conditions in which the applied point loads are simply replaced by pure torsional loads. This mathematical idealization neglects some practical factors, such as specimen end and shape effects, loading point irregularity, mode II interference, and possible friction, etc. For an actual ECT test these

factors could have significant effects on the results and these effects must be assessed. A comprehensive analysis is necessary to evaluate these effects and examine the validity and accuracy of analytical models for this test configuration.

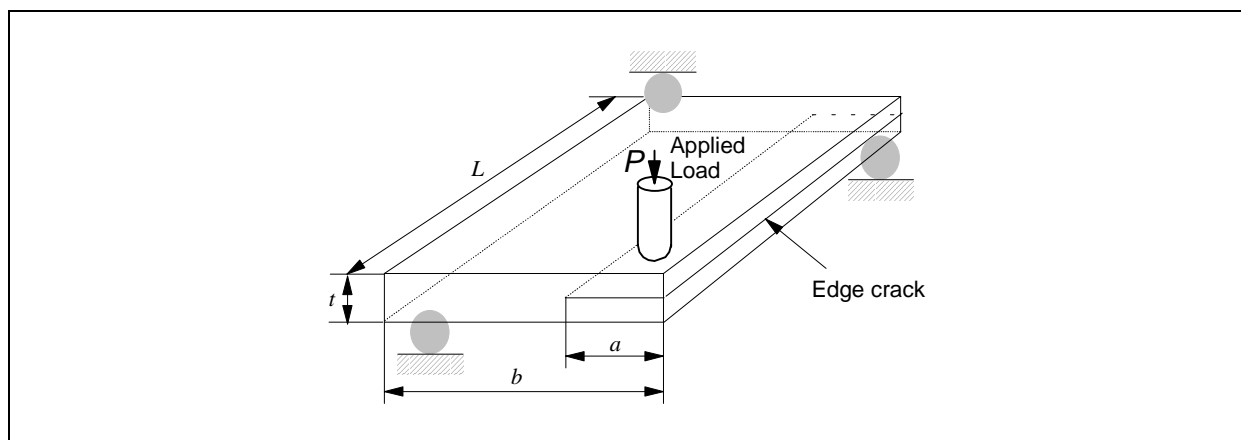


Figure 1. The edge crack torsion (ECT) test configuration.

In this study, a three-dimensional (3-D) finite element analysis was performed on a class of $[90, (+45/-45)_n, (-45/+45)_n, 90]_s$ laminated composites under the edge crack torsion (ECT) test configuration. Finite element delamination models were established from which the mode III fracture toughness of the composites was calculated. The relations between the interlaminar fracture behavior and various configuration parameters were investigated and the effects of point loading, ends, geometry, mode II interference, and friction were evaluated.

An experimental investigation of the ECT test was also conducted on the class of $[90, (+45/-45)_n, (-45/+45)_n, 90]_s$ carbon/epoxy laminated composite samples to verify the analysis methods and improve the test procedure. A new two-point loading fixture was fabricated which was simpler and more versatile than the one-point loading fixture for the ECT test. This improved ECT test was carried out on the specimens with $n = 2, 3$, and 4 layups. The results obtained from the test were consistent with those predicted by the finite element analysis. A procedure for specimen layup/crack length selection for a valid ECT mode III test was proposed.

FEM ANALYSIS [5]

The study reported in this paper aimed at performing a complete analysis using the 3-D finite element method for the actual ECT specimen configuration and eventually validating analysis methods towards an effective mode III delamination test. Technically, the tasks to be performed include: (1) Establishment of 3-D fracture models with different types of elements combined together to describe the attributes and features of the real ECT specimens; (2) Creation of 3-D collapsed quarter-point singular elements to capture the mode III crack front singularity; (3) Convergence and accuracy study to validate the models and to optimize for efficiency; (4) Development of the virtual crack closure method to calculate G_{III} from the 3-D FEM results for laminated composite specimens; and (5) Calculations to investigate parameter effects of specimen ends, point loads, mode II component, specimen dimension ratios, and friction, etc.

Due to the nature of out-of-plane deformation for the ECT specimen configuration 3-D finite element modeling was necessary and actually used in this study. The models to be established were designed to possess the features with prescribed layup, orthotropic ply properties, sandwiched mid-plane edge crack, and asymmetric loading conditions, etc. The modeling is illustrated in Figure 2:

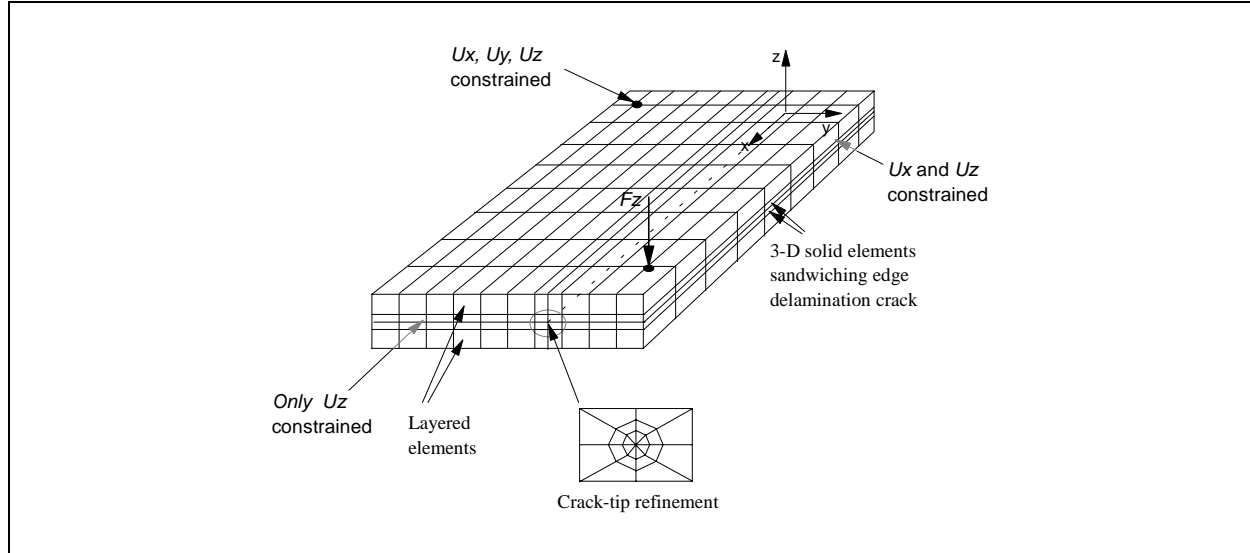


Figure 2. FEM meshing and boundary conditions for the ECT configuration

The finite element calculation was performed using the ANSYS50 program on an Intel based personal computer. Both interactive and batch modes were used. The interactive mode was employed primarily in the preprocessing and post-processing phases for model and result displays. Batch processing was adopted for the program execution of the entire calculation procedure.

Four types of elements were used in the finite element modeling to best describe the features of the real ECT specimen configuration. SOLID45 are the simplest 3-D isoparametric solid elements defined by 8 nodal points having three degrees of freedom (DOF) at each node and with the orthotropic material properties. They were used as non-singularity elements for meshing most of or the entire two midplane plies containing the edge crack. SOLID95 are the more complicated 3-D isoparametric solid elements, defined by 20 nodal points. They were used for meshing the vicinity of the crack front only when establishing the singularity element model, which is described in the following sections. SOLID46 are the layered solid elements defined by 8 nodal points and featured with laminate properties and orthotropic material properties for each ply. They were used for modeling the major part of the laminated composite specimen. CONTAC52 are the 3-D interface elements defined by 2 nodal points with the only material property being the frictional coefficient. It was used for simulating the contact and frictional sliding between the upper and lower crackfaces.

The orthotropic material properties were required by either 3-D solid or layered elements in this FEM computation. For such materials there is no coupling between normal and shear deformation, namely a shear stress does not cause any normal strains and a normal stress does not cause any shear strains. Therefore, there are nine independent constants that can be defined

as E_{11} , E_{22} , E_{33} , G_{12} , G_{13} , G_{23} , ν_{12} , ν_{13} , and ν_{23} under the three symmetric material axes 1, 2, and 3. For the specific ECT specimens which were composed of unidirectional plies with transversely isotropic material properties, the number of material constants becomes seven because $E_{22}=E_{33}$ and $G_{12}=G_{13}$ if axis 1 is defined along the fiber longitudinal direction and axes 2 and 3 in the transverse directions. The material properties used in the FEM calculation are: $E_{11}=165\text{GPa}$, $E_{22}=E_{33}=10.3\text{ GPa}$, $G_{12}=G_{13}=5.5\text{ GPa}$, $G_{23}=4.0234\text{ GPa}$, $\nu_{12}=\nu_{13}=\nu_{23}=0.28$, and $\nu_{21}=0.01748$. The layered solid composite elements (SOLID46) were defined by node positions and laminate properties (ply thickness, orientation, and layups).

The most important region in a fracture or delamination model is the region around the edge of the crack, which is referred to as a crack tip in a 2-D model and a crack front in a 3-D model. For this 3-D ECT modeling, since the same meshing patterns were used in any y - z planes along the delamination front (x -direction), the crack-tip region, as shown in Figure 2, was taken into account. As illustrated in this figure, the original mesh in the crack-tip vicinity consisted of only four elements with the size $0.2 \times 0.13\text{ mm}$ comparable to the thickness of the whole layer of elements. This coarse mesh could not pick up the sharply varied stress and strain distributions near the crack tip. A fine mesh in this region was needed.

In finite element delamination modeling, a proper treatment of delamination faces is essential for a reliable calculation. For this specific configuration, crackface crossover may happen if the top and bottom halves of the specimen are allowed to deform freely without any restraint. A coupled DOF in the z -direction, U_z , was imposed on the adjacent pairs of nodes between the crackfaces to prevent such crossover.

Based on the calculation results obtained from the finite element fracture models, the strain energy release rates, G , can be calculated using the following equations derived by extension of Irwin's virtual crack closure technique (VCCT) [6,7]:

$$G_I = -\frac{1}{2\Delta_x\Delta_y}[F_{zi}(w_j - w_{j'})] \quad (2.1)$$

$$G_{II} = -\frac{1}{2\Delta_x\Delta_y}[F_{yi}(v_j - v_{j'})] \quad (2.2)$$

$$G_{III} = -\frac{1}{2\Delta_x\Delta_y}[F_{xi}(u_j - u_{j'})] \quad (2.3)$$

where Δ_x and Δ_y are the x - and y -dimensions of the crack-front elements, F_{xi} , F_{yi} , and F_{zi} are the nodal forces at node i in the x -, y -, and z -directions, calculated from all elements in the upper half of the model adjacent to node i , $(u_j - u_{j'})$, $(v_j - v_{j'})$, and $(w_j - w_{j'})$, are the relative displacements at the node pair j and j' in the x -, y -, and z -directions, as shown in Figure 3. These calculated G values represented the strain energy release rate components at point i on the delamination front.

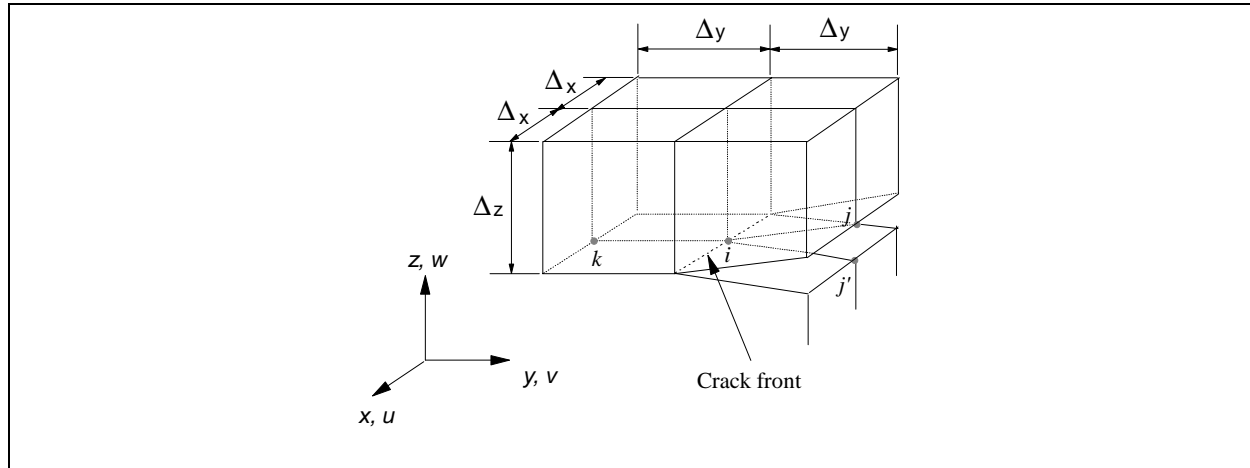


Figure 3. Non-singular elements at crack front used for calculation of G at node i .

ECT TEST

The ECT test was performed on carbon/epoxy composite samples for measuring the mode III interlaminar fracture toughness. A CIBA-GEIGY epoxy resin system R6376 reinforced with IM6 (Hercules) carbon fibers was selected for this study. The unidirectional prepreg tape was developed for use in the design and fabrication of primary aircraft structures with excellent retention of high fiber breaking strains. The carbon/epoxy composite system was in the form of prepreg tape of 254 mm wide roll, with a fiber areal weight of 145g/m².

The prepreg tape was first cut into pieces of about 290 mm long and 140 mm wide, with the fiber orientation angles 90, +45, and -45 with respect to the sample longitudinal direction. The correct number of prepreg layers were stacked together to form the desired layups. Two strips of Teflon[®] film, approximately 40 mm wide and 10 μm thick, were placed in the mid-plane of the laminate during layup to introduce initial cracks in the specimens. Then the laminate panel was put in a vacuum bag in an autoclave. After a total of about 4 hours curing in autoclave conditions under the prescribed curing cycle (raise temperature at 2.8°C per minute straight up to 177°C with 0.7 MPa autoclave pressure; hold temperature at 177°C for 120 minutes; cool under pressure down to 60°C), the laminate panel was removed from the vacuum bag and later cut into ECT specimens of about 88.9 mm long and 38.1 mm wide with the edge crack introduced by the Teflon insert. Each laminate panel could be cut into three sets of specimens and each set contained three specimens with the same crack length. The crack lengths for all specimens ranged from 13 to 25 mm.

The ECT specimens were tested under ambient conditions (approximately 20°C and 65% RH) using a computer-controlled Instron 5567 tester with a 10 kN load cell and a specially designed two-point loading fixture. The fixture consisted of a steel supporting plate (153 x 101 x 25 mm) on which two 12.7 mm diameter balls were attached for the fixed supports, and a steel bar (180 x 25 x 25 mm), with 2 loading balls, attached to the testing machine crosshead, as shown in Figure 4. The controlled crosshead speed was 2 mm per minute. Instantaneous load, P , and crosshead displacement, δ , were recorded at a rate of one data pair per second. Under the two-point loading configuration, the actually applied load at each loading point is $P/2$, and the deflection at both loading points has the same value as δ .

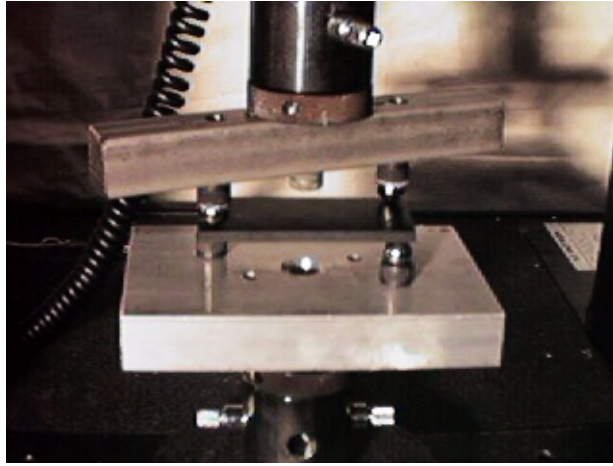


Figure 4. Set-up for the ECT delamination test

RESULTS AND DISCUSSION

Typical distributions of strain energy release rate components for the $n=2$ layup specimens are shown in Figure 5, in which clear local irregularities near the point loads can be identified, the effective range where G_{III} is near constant, can be determined for calculating the critical G_{III} value.

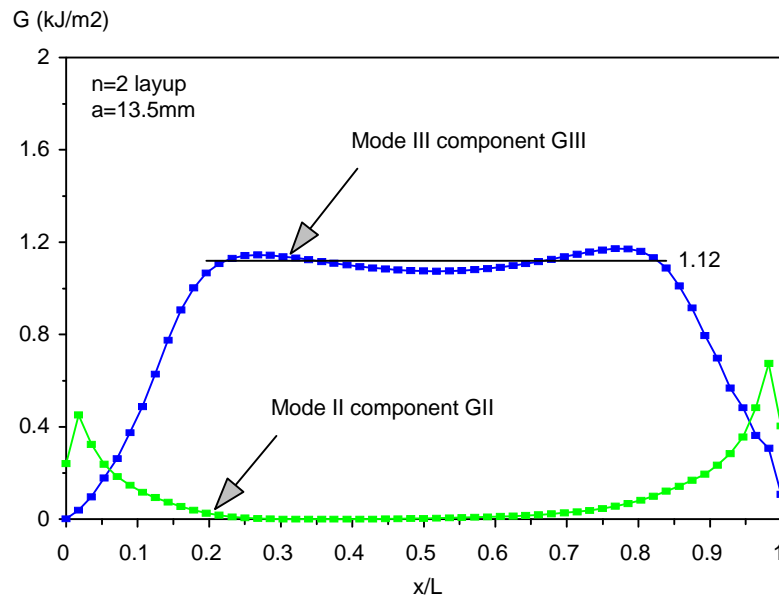


Figure 5. Typical distributions of strain energy release rates for $n=2$ layup.

The finite element analysis showed that with proper selection of specimen configuration and layup, the delamination could grow in pure Mode III at the middle region of the specimen

length away from the ends. An effective range was defined to describe the middle region where the Mode III strain energy release rate G_{III} were near constant. The critical strain energy release rate component G_{III} averaged over the effective range along the delamination front was comparable with the experimental data determined using the compliance calibration method from the ECT test.

A Mode II component G_{II} was found to exist in the end regions in which the supporting and loading points were located. The magnitude of the Mode II strain energy release rate component at the loading point was much smaller than that of the Mode III component in the mid-section of the specimen, and therefore, the Mode II component did not interfere significantly with the Mode III delamination state which would dominate the behavior of the specimen under the actual test configurations. However, the Mode II interference could become significant with changes of configuration parameters such as the loading condition and the specimen geometry.

The point-load local effect was found to be insignificant, especially for specimens with thicker layups ($n=4$). Specimen end size, dimension ratio, layup, and crack length were found to have significant effect on the interlaminar fracture behavior and the calculated strain energy release rates. Friction between the delamination faces showed negligible effect on the calculated strain energy release rates, and thus it can be neglected in the ECT test.

The experimental study on the edge crack torsion (ECT) test was conducted using carbon/epoxy laminated composite samples for verifying analysis methods and improving the test procedure. The ECT test was carried out on the specimens with the $n = 2, 3$, and 4 layups. Some typical test curves are shown in Figure 6. Critical load corresponding to delamination propagation is identified from the test curve where the curve becomes nonlinear. The crack length and layup effects were analyzed using the test results. Results show that the calculated G_{IIIc} values are insensitive to the crack lengths for all three layups: $n = 2, 3$, and 4, suggesting that the crack length has insignificant effect on the calculated fracture toughness G_{IIIc} .

Specimen layups have many effects on the test and the results. Generally, a thicker layup ($n=4$) is favored for higher torsional stiffness and for less point load irregularities. The results obtained from the test agreed well with the findings from the finite element analysis.

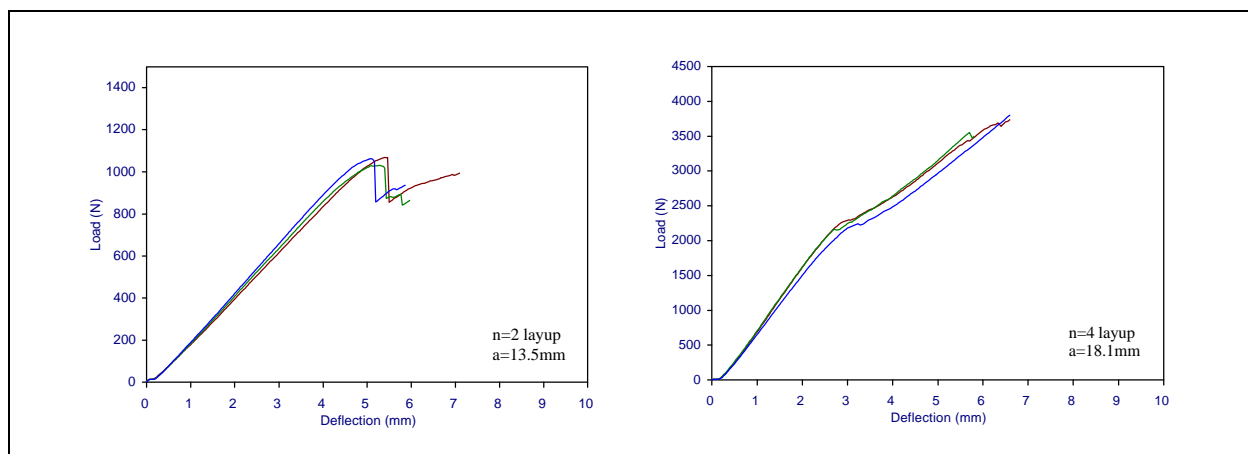


Figure 6. Typical ECT test curves for specimen with the $n=2$ and $n=4$ layups

CONCLUSIONS

A 3-D finite element analysis was performed on laminated composites under the ECT test configuration for characterization of Mode III delamination. Finite element delamination models were established and formulas for calculating the Mode III fracture toughness from 3-D finite element models were developed. The relations between the interlaminar fracture behavior and various configuration parameters were investigated including the effects of point loading, specimen ends, geometry, Mode II interference, and friction. These effects are quantified in the analysis.

An experimental study on the edge crack torsion (ECT) test using the new two-point loading fixture, which demonstrated certain advantages over the one-point loading fixture for the ECT test. The crack length and layup effects were analyzed using the test results. Results show that the crack length does not significantly affect the calculated fracture toughness G_{IIIc} .

REFERENCES

1. Lee, S. M., "An Edge Crack Torsion Method for Mode III Delamination Fracture Testing," *Journal of Composites Technology & Research*, Vol. 15, No. 3, Fall 1993, pp. 193-201.
2. Li, J. and Wang, Y., "Analysis of a Symmetric Laminate with Mid-Plane Free Edge Delamination Under Torsion: Theory and Application to the Edge Crack Torsion (ECT) Specimen for Mode III Toughness Characterization," *Engineering Fracture Mechanics*, Vol. 49, No. 2, 1994, pp. 179-194.
3. Li, J. and Wang, Y., "Analysis of Mode III Delamination Fracture Testing Using a Mid-Plane Edge Crack Torsion Specimen," in *Composite Materials: Testing and Design*, Vol. 12, ASTM Standard Technical Publication STP 1274, R.B. Deo and C.R. Saff, eds., ASTM, West Conshohocken, PA, 1996, pp. 166-181.
4. Li, J., Lee, S.M., Lee, E.W., and O'Brien, T.K., "Evaluation of the Edge Crack Torsion (ECT) Test for Mode III Interlaminar Fracture Toughness of Laminated Composites," *Journal of Composites Technology & Research*, Vol. 19, No. 3, 1997, 174-183.
5. Zhao, D. and Wang, Y., "Finite Element Analysis of Mode III Fracture Behavior of Laminated Composites under Edge Crack Torsion Test Configuration," *Theoretical and Applied Fracture Mechanics*, Vol. 29, No. 2, 1998.
6. Hellen, T. K., On the Method of Virtual Crack Extension, *International Journal for Numerical Methods in Engineering*, Vol. 9, 1975, pp. 187-207.
7. Rybicki, E. F. and Kanninen, M. F., A Finite Element Calculation of Stress Intensity Factors by a Modified Crack Closure Integral, *Engineering Fracture Mechanics*, Vol. 9, 1977, pp. 931-938.